Cobalt effects on prokaryotic communities of river biofilms: Impact on their colonization kinetics, structure and functions

Sarah Gourgues, Marisol Goñi, Mathieu Milhe-Poutingon, Patrick Baldoni-Andrey, Nicholas Bagger Gurieff, Clémentine Gelber, Séverine Le Faucheur

Science of the Total Environment 951 (2024) 175713

Contents lists available at ScienceDirect

Science of the Total Environment

journal homepage: www.elsevier.com/locate/scitotenv

Cobalt effects on prokaryotic communities of river biofilms: Impact on their colonization kinetics, structure and functions

Sarah Gourgues [a,*], Marisol Goñi-Urriza [a], Mathieu Milhe-Poutingon [a], Patrick Baldoni-Andrey [b], Nicholas Bagger Gurieff [c], Clémentine Gelber [b], Séverine Le Faucheur [a]

[a] Universite de Pau et des Pays de l'Adour, E2S-UPPA, CNRS, IPREM, Pau, France
[b] TotalEnergies, Pôles d'Études de Recherche de Lacq, France
[c] Rio Tinto, Closure R&D, Brisbane, Queensland, Australia

HIGHLIGHTS

- Co accumulation in growing biofilms was correlated with Co ambient concentrations.
- The Co exposure affected prokaryotic community structure from the earliest stages of colonization.
- Co induced a change in the potential carbon fixation in exposed biofilms.
- No structural resilience was observed in biofilms after cessation of Co exposure.

GRAPHICAL ABSTRACT

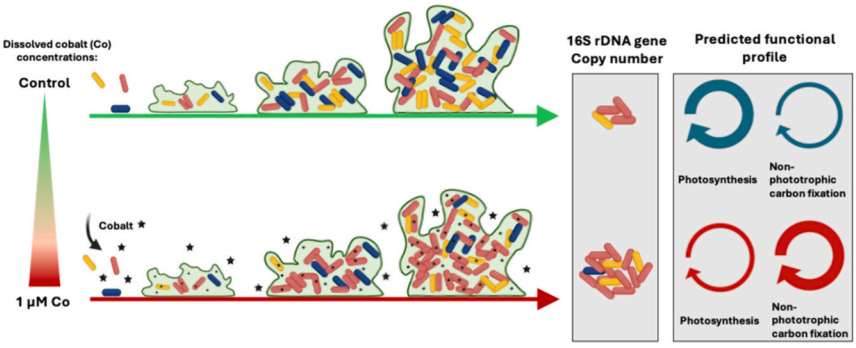

ARTICLE INFO

Editor: Sergi Sabater

Keywords:
Microbial ecotoxicology
Bioindication
Metabarcoding
Metal
Microbial communities

ABSTRACT

Although cobalt (Co) plays a significant role in the transition to low-carbon technologies, its environmental impact remains largely unknown. This study examines Co impacts on the prokaryotic communities within river biofilms to evaluate their potential use as bioindicators of Co contamination. To this end, biofilms were cultivated in artificial streams enriched with different environmental Co concentrations (0.1, 0.5, and 1 µM Co) over 28 days and examined for prokaryotic abundance and diversity via quantitative PCR and DNA-metabarcoding every 7 days. The prokaryotic community's resilience was further investigated after an additional 35 days without Co contamination. The prokaryotic communities were affected by 0.5 and 1 µM Co from the onset of biofilm colonization. The biofilm biomass was comparable between treatments, but the community composition differed. Control biofilms were dominated by *Cyanobacteria* and *Planctomycetes*, whereas *Bacteroidetes* dominated the Co-contaminated biofilms. Potential functional redundancy was observed through the implementation of

Abbreviations: Co, cobalt; DOC, dissolved organic carbon; EDTA, ethylenediaminetetraacetic acid; EPS, extracellular polymeric substance; FROGS, find rapidly OTUs with galaxy solutions; KEGG, Kyoto Encyclopedia of Genes and Genomes; NMDS, non-metric multi-dimensional scale; NSTI, nearest-sequenced taxon index; OTU, operational taxonomic unit; PGTB, Plateforme Génome Transcriptome de Bordeaux; PNEC, predicted no-effect concentration; STAMP, Statistical analysis of metagenome profiles; WHAM, Windermere Humic Aqueous Model.

* Corresponding author at: Universite de Pau et des Pays de l'Adour, E2S-UPPA, CNRS, IPREM, Technopôle Hélioparc, 2 Av. Du Président Pierre Angot, 64053 Pau Cedex 9, Pau, France.
E-mail address: Sarah.gourgues@univ-pau.fr (S. Gourgues).

https://doi.org/10.1016/j.scitotenv.2024.175713
Received 16 May 2024; Received in revised form 19 August 2024; Accepted 21 August 2024
Available online 25 August 2024

carbon fixation alternatives by non-photosynthetic prokaryotes in biofilms exposed to high Co concentrations. No structural resilience was observed in the biofilms after 35 days without Co contamination. Measuring the prokaryotic community structural response using molecular approaches appears to be a promising method for assessing shifts in water quality owing to Co contamination.

1. Introduction

In the context of energy transition, cobalt (Co) has emerged as a metal of interest in the production of batteries. The surge in demand for lithium-ion batteries, particularly for vehicles and electronic devices, led to a remarkable increase in its extraction (+95%) and use (quadrupled) between 2008 and 2018 (Graedel and Miatto, 2022; U.S Geological Survey, 2008, 2018). Consequently, Co has been frequently detected in aquatic systems at potentially concerning concentrations, particularly near industrial sites (Banza Lubaba Nkulu et al., 2018; Barrio-Parra et al., 2018). Background dissolved Co concentrations in European freshwater environments typically range between 0.17×10^{-3} and 0.27 μM Co (average $5.65 \times 10^{-3} \pm 0.02$ μM Co, $n = 807$) (Batista et al., 2005), though concentrations as high as 53 and 48 μM Co have been measured in mining effluents in the Democratic Republic of Congo and near Spanish industrial plant discharges, respectively (Atibu et al., 2013; Banza Lubaba Nkulu et al., 2018; Barrio-Parra et al., 2018; Batista et al., 2005).

Cobalt is an essential micronutrient for organisms at trace levels (nM) and is a significant co-factor in numerous enzymatic processes as the main constituent of vitamin B12 (Allen, 2012; Facey et al., 2022; Martens et al., 2002). However, studies conducted on model microorganisms have demonstrated its toxicity at higher concentrations. For instance, the model bacterium *Geobacter sulfurreducens* strain PCA exhibited longer generation times when grown at Co concentrations equal to or exceeding 250 μM (Dulay et al., 2020). Minimum inhibition concentrations of Co have been reported to range between 400 and 800 μM for several strains of *Pseudomonas* sp. and at 200 μM for *E. coli* (Hassen et al., 1998; Gikas, 2008). Similar inhibition concentrations were identified for *Pseudomonas aeruginosa* strain PU21 (EC20 = 460 μM Co) (Chen et al., 2006), while the growth of the unicellular cyanobacterium *Anacystis nidulans* was entirely inhibited above 509 μM Co (Lee et al., 1992). More recently, a study evaluating the effects of lithium, nickel, manganese and cobalt oxide showed that Co^{2+} ions at 3.4 μM with 7.7 μM of Ni^{2+} ions noticeably affected the respiration of the model strain *Shewanella oneidensis* MR-1 (Hang et al., 2016). Negative impacts have also been reported in microalgae (Li et al., 2007). A decrease in pigment content and growth rates has also been observed in microalgae in the presence of Co at concentrations equal to or >17 μM (El-Sheekh et al., 2003; Fawzy et al., 2020).

Aquatic biofilms are aggregate forms of microbial life that develop on submerged substrates. These assemblages include a wide variety of microorganisms – such as bacteria, archaea, microalgae, fungi, and meiofauna – embedded in an extracellular polymeric substance (EPS) matrix (Besemer, 2016; Flemming and Wingender, 2010). Nowadays, biofilms are widely used in biomonitoring due to their interesting features that allow them to serve as early warning systems for disturbances in aquatic ecosystems (Sabater et al., 2007). They are ubiquitous, easy to collect, and have a sedentary lifestyle. Aquatic biofilms also have a rapid life cycle, enabling them to act as integrative bioindicators for water quality changes. Their ability to bioaccumulate contaminants also provides information about the bioavailability and toxicity of contaminants (McGeer et al., 2004). Lastly, their position at the base of the trophic chain is vital to study potential repercussions on interactions between biofilm components and higher trophic levels (Guasch et al., 2016). Numerous ecotoxicological studies have examined the effects of metals, pesticides, and emerging compounds on biofilms (Guasch et al., 2016). The long-term consequences of metal pollution on biofilms in water quality restoration contexts have also been investigated (Arini et al., 2012; Lawrence et al., 2004).

To date, only a few studies have examined the impact of Co on biofilms. Cobalt bioaccumulation has been linked to a disruption in the synthesis of chlorophyll *a* and the growth of biofilms when present at 85 and 17 μM, respectively (Dutta et al., 2022). In Co-contaminated waters, prokaryotic and microeukaryotic communities, along with the metametabolome from mature biofilms translocated in Co contaminated waters, were quickly affected (within hours) (Colas et al., 2024). Following translocation, there was a decrease in the relative abundance of the major phylum *Planctomycetota*, while *Alphaproteobacteria* rapidly increased. An increase in the phylum *Cyanobacteria* was also observed in biofilms exposed to 1 μM Co after 28 days of exposure. These studies, however, focused on mature biofilms and did not investigate Co impact on biofilm first stages of biofilm colonization and establishment in the presence of Co. Previous research has reported the high vulnerability of biofilms during the early stages of colonization when exposed to metals such as Cd (Ivorra et al., 2000) or TiO_2 nanoparticles (Li et al., 2020).

Although a few studies have demonstrated Co toxicity to microorganisms exposed to environmentally relevant concentrations, the potential impacts on rivers remain unclear, and environmental quality standards (EQS) are rarely available. The Canadian legislation is the only one to have implemented a site-specific Federal Water Quality Guideline to protect aquatic life, set at 0.01 μM Co for waters with a hardness of 100 mg/L (Environment Canada, 2017). By contrast, no EQS is available in Europe or the United States. However, Co has recently been classified as a relevant substance to monitor in continental waters within France (Institut National de L'environnement Industriel et Des Risques, 2022). The European Chemicals Agency has calculated the predicted no-effect concentration (PNEC) of Co at 0.02 μM (1.06 μg L^{-1}) in freshwaters (European Chemicals Agency, 2023).

Biofilms are commonly used in ecotoxicology, with much of the research centered on microalgal communities. Indices that are based on diatom abundance and diversity are now included in numerous water quality monitoring programs around the globe, such as the Water Framework Directive in Europe (Coste et al., 2009), and similar initiatives in Canada and the USA. Despite the potential to implement a multilevel approach when evaluating biofilms, the prokaryotic component has received less attention for its potential as a bioindicator of water quality degradation. In 2007, the International Union of Pure and Applied Chemistry (IUPAC) defined a biological indicator as: '*a species or group of species that is representative and typical for a specific status of an ecosystem, which appears frequently enough to serve for monitoring, and whose population shows a sensitive response to changes (e.g., the appearance of a toxicant in an ecosystem)*' (Duffus et al., 2007). Prokaryotes are known for their quick response to environmental changes, including alterations in metal concentrations (Pal et al., 2022). They also offer a variety of ecosystem services, including those at the biofilm level. For instance, auto- and heterotrophic organisms are closely connected, and their metabolic cooperation is crucial for the cycling of major elements (Battin et al., 2016). This interdependence among communities characterizes biofilms as a functional consortium, where stresses can affect the overall microecosystem structure and function. The enhancement of molecular techniques over the last few decades, along with the continual refinement of 16S rDNA gene reference databases, has led to a more comprehensive understanding of prokaryotic responses to stress, encompassing both the community structure and functional profile. As a result, prokaryotes can offer different levels of bioindication within biofilms.

The current study aimed to investigate the ecotoxicological effects of

Co on prokaryotic communities within river biofilms and to evaluate whether the response of these communities in terms of their structure and composition can be used as a suitable endpoint for bioindication of Co contamination. Biofilms were grown in artificial streams polluted with Co and examined to determine changes in the abundance, structure, and functional potential of the prokaryotic community after 7, 14, 21, and 28 days of colonization. This included a physico-chemical analysis of the water composition. Additionally, the resilience of the prokaryotic community in exposed biofilms was examined following the restoration of natural water quality for 35 days.

2. Material and methods

2.1. Exposure experiments and sample collection

Exposure experiments were conducted in outdoor artificial streams at the Pilot Rivers facilities (TotalEnergies, Lacq, France). The artificial streams were filled continuously from the Gave de Pau River, without any pre-treatment, at a flow rate of 7.5 $m^3\ h^{-1}$ (Fig. A.1). Cobalt (Co(II) chloride hexahydrate, 98%, Thermo Scientific Chemicals) was added to nine streams to achieve nominal concentrations of 0.1, 0.5, and 1 μM, in triplicate (3 treatments × 3 streams). These Co concentrations were 5 to 55 times higher than the PNEC (0.02 μM) (European Chemicals Agency (ECHA), 2023), thus representing environmentally relevant concentrations. Three additional streams served as control environments, which were filled only with Gave de Pau water, without any Co addition.

At the beginning of the exposure experiments (Day 0), 13 sterile glass slides (10 × 20 cm) were placed in each stream as a substrate for biofilm colonization. Water and biofilm were collected every 7 days during biofilm colonization (D7, D14, D21, and D28), and 35 days following the cessation of Co injection (D63). For every sampling event during Co exposure, biofilm samples were collected into 2 mL sterile Eppendorf tubes by scraping three slides from each channel using sterile microscope slides. However, only one slide was utilized at D63. Detailed illustrations of the glass slides collected for biofilm sampling are presented in Fig. S2. Samples were weighed and stored at −80°C for molecular analyses and at −17°C for chlorophyll content and bioaccumulation analyses. Biofilms dry weight and chlorophyll content were measured for each sample (more detailed protocols are provided in Text S2).

On the day of sample collection, the physico-chemical parameters of the water – namely, pH, temperature, dissolved oxygen, and conductivity – were measured in each stream. Water was also collected and stored at 4°C for measuring alkalinity, dissolved cations (including Co), anions, and organic carbon concentrations (Text S1). Cobalt speciation was calculated using the Windermere Humic Aqueous Model (WHAM, version 7.05.5) (Bryan et al., 2002; Tipping, 2007).

2.2. Cobalt bioaccumulation

Total and intracellular bioaccumulated Co were measured in freeze-dried biofilms that had been mineralized with a mix of 70 % nitric acid (Metal grade, Sigma-Aldrich, Germany) and 30 % hydrogen peroxide (H_2O_2; Ultra trace, Sigma-Aldrich, Germany, 2:1 v/v ratio) in an UltraWAVE oven (Milestone, Italy). For intracellular analysis, fresh biofilms were initially rinsed with 10 mM of ethylenediaminetetraacetic acid (EDTA ≥99%, Sigma-Aldrich, Germany) for 10 min, and then rinsed with filtered (0.45 μM) water from the control stream of Pilot Rivers (Colas et al., 2024; Meylan et al., 2004). Cobalt concentrations in the mineralized biofilms were measured using an ICP-MS (Agilent ICP-MS 7500, CA, USA). A certified standard reference material (BCR-414) (Plankton, JRC, Brussels) was used to confirm the digestion of biofilm (recovery of 86.3 ± 8.6%, $n = 6$).

2.3. Diversity and functional potential of the prokaryotic community under Co contamination

DNA extractions were carried out using the PowerSoil DNA Isolation Kit (Qiagen, Germany), following the manufacturer's instructions. The extracted DNA was quantified using a Qubit 1X dsDNA BR assay kit (ThermoFisher Scientific, USA). The V4-V5 hypervariable regions of the 16S rDNA gene were sequenced post-amplification with the universal primers V4-515F and V5-928R (Wang and Qian, 2009). Detailed PCR protocols can be found in Text S3. Amplicons were subsequently sequenced by La Plateforme Génome Transcriptome de Bordeaux (PGTB, Bordeaux, France) using the Illumina Miseq 2 × 300 pb method and reagent kit V3. The raw sequences can be accessed in the National Center for Biotechnology Information's Sequence Read Archive under the accession number PRJNA1098091.

Raw sequences were processed using the FROGS (version 4.1.0) pipeline (Find Rapidly OTUs with Galaxy Solution) (Escudié et al., 2018). The raw sequences were merged, denoised, and dereplicated using the VSEARCH tool (Rognes et al., 2016). Sequences shorter than 200 bp were removed for further analysis. Clustering into operational taxonomic units (OTUs) was conducted with Swarm (Mahé et al., 2014), setting the aggregation distance clustering to 1. Chimeras and OTUs that represented <0.005% of all sequences were also removed (Bokulich et al., 2013). Data was normalized to 10,675 reads per sample and the final total number of OTUs was 1,437. Taxonomic assignments of OTUs were performed using 16S SILVA 138.1 and OTUs associated with chloroplasts were removed for further analysis.

The predicted functional profiles of communities, based on 16S sequences, were inferred by using PICRUSt2 (Douglas et al., 2020). Sequences with the nearest-sequenced taxon index (NSTI) exceeding the default cutoff of 2 were excluded. The resulting metabolic profiles were then annotated using the Kyoto Encyclopedia of Genes and Genomes (KEGG) pathways with the ggpicrust2 package (Yang et al., 2023) in RStudio.

2.4. Quantification of the 16S rDNA gene

The copy number of the 16S rDNA gene was quantified using the DyNAmo Flash SYBR Green qPCR Kit (ThermoFisher Scientific, USA) with the same primer pairs used for microbial diversity analysis (referenced above) but without MiSeq adaptors. More detailed qPCR protocols can be found in Text S4. Absolute quantification was carried out with homemade standards consisting of pGEM cloned amplicons of the *Escherichia coli* 16S rDNA gene. The analyses were processed in triplicates for each biological replicate. The PCR efficiency was assessed at 96%.

2.5. Statistical analyses

Alpha diversity metrics, namely, species richness, diversity (Shannon index), and evenness (Pielou index), were calculated using the Vegan package in RStudio (Oksanen et al., 2022). Additionally, the Chao1 index was computed in FROGS (version 4.1.0) to account for rare OTUs (Escudié et al., 2018). All comparisons were executed in RStudio using ANOVA and Tukey post-hoc tests, where applicable. If the conditions for application were not met, a non-parametric approach was adopted, entailing the use of Kruskal-Wallis and subsequent Dunn post-hoc tests. Beta-diversity was assessed with non-metric multi-dimensional scaling (NMDS) based on Bray-Curtis dissimilarity distances between OTU. Significant differences between communities were evaluated by a permutational multivariate analysis of variance (PERMANOVA) using the Vegan package, followed by pairwise comparisons employing the pairwiseadonis2 package (Martinez Arbizu, 2020). Comparisons between proportions of taxonomic groups (representing more than >1% of the community) and functional pathways derived from PICRUSt2 analysis were carried out using the statistical analysis of metagenomic

profiles (STAMP) (Parks et al., 2014), utilizing White's non-parametric test and an effect size filter for proportion differences exceeding 1%.

3. Results

3.1. Physico-chemical parameters of waters

The physico-chemical parameters of the water remained stable throughout the experiment, except for the water temperature, which decreased from 14.30 ± 0.12°C (Day 7) to 8.17 ± 0.03°C (Day 63) (Table S1). In the control streams (n = 3), the average dissolved Co concentration was 4.62 ± 4.02 nM. The average Co concentrations over the 28 days of exposure aligned with the nominal concentrations (0.092 ± 0.004, 0.525 ± 0.084, and 1.089 ± 0.07 μM, respectively) (Table S1). Cobalt was predicted to be primarily complexed by carbonates ($CoCO_3$) and in its free form (Co^{2+}), accounting for 53 ± 3% and 29 ± 2% of the total dissolved Co, respectively; the proportion of Co bound to fulvic acids was only 0.83 ± 0.51% (Table S1). After the Co injection was stopped, the dissolved Co concentration returned to its natural level in all streams.

3.2. Co accumulation

Both total and internalized bioaccumulated Co displayed a positive correlation with free Co^{2+} concentrations, exhibiting significant linear relationships (Fig. 1 and Table S2). Throughout the experiment, total bioaccumulated Co in both control and exposed biofilms remained stable, regardless of the Co exposure concentration (Fig. S3-A; Table S2). However, the amount of internalized Co increased over time in Co-exposed biofilms ($p < 0.05$) (Fig. S3-B). These increases reached 3.47 ± 1.63 μmol Co.g^{-1} DW for biofilms exposed to 0.1 μM of Co, 4.23 ± 0.25 μmol Co.g^{-1} DW for biofilms exposed to 0.5 μM and 7.68 ± 1.10

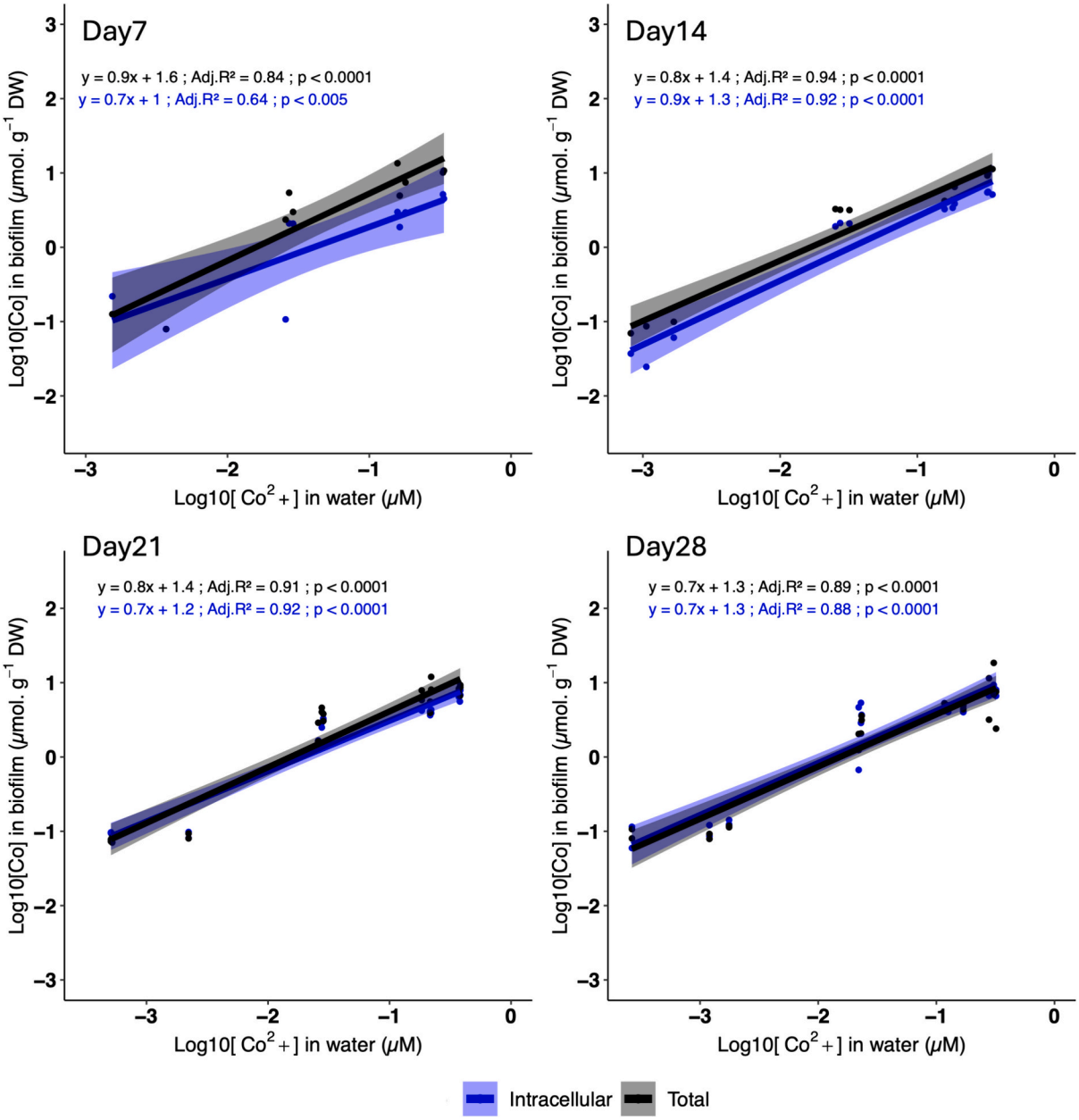

Fig. 1. Bioaccumulation of cobalt in biofilms over the colonization period. Lines represent regressions of total bioaccumulated Co (**black**) and internalized Co (**blue**) as a function of free ion Co^{2+} concentration in the exposure medium at each sampling time. The shaded areas represent the confidence intervals (95 %) around the associated line.

μmol Co.g^{-1} DW for biofilms exposed to 1 μM at D28. At D63, the bioaccumulated Co decreased in the exposed biofilms ($p < 0.05$), but the Co levels remained between 4.35 and 8.68 times higher than those found in control biofilms ($p < 0.05$) (Fig. S3-A;C).

3.3. Biofilm structure as a function of Co exposure

The biofilms (dry biomass) grew over the colonization period with significant increases observed between D7 and D21, followed by stabilization after the latter day. This remained consistent irrespective of the Co exposure conditions (Fig. 2A, Table S3). In both the control and exposed biofilms, the levels of chlorophyll *a*, *b*, and *c1* + *c2* displayed an upward trend (Fig. 2B and Table S3). Biofilms exposed to 1 μM of Co at D21 and D28 had a higher chlorophyll *b* content than either the control or biofilms that were exposed to 0.1 μM ($p < 0.05$). Conversely, as Co exposure concentrations rose, the content of chlorophyll *a* and *c1* + *c2* decreased, with significantly reduced levels in biofilms exposed to 0.5 μM Co compared with the control (Figs. 2B, S3).

3.4. Prokaryotic abundance and diversity in biofilms cultivated under Co contamination

The copy number of the 16S rRNA gene (used as a proxy for prokaryotic abundance) increased in all biofilms between D7 and D14 ($p < 0.01$), regardless of Co concentration (Fig. 2C, Table S6). After D14, the abundance of prokaryotes in control and 0.1 μM-exposed biofilms remained stable, but significantly increased when exposed to 0.5- and 1 μM of Co ($p < 0.05$). At D21, biofilms exposed to 0.5- and 1 μM had 3-fold higher levels of 16S rRNA gene copy numbers than the control or 0.1 μM-exposed biofilms ($p < 0.05$). 16S rRNA gene copy numbers significantly decreased between D28 and D63 for all biofilms ($p < 0.005$). Nevertheless, after the cessation of Co exposure at D63, the prokaryotic abundances of biofilms previously exposed to 0.5 μM and 1 μM of Co remained higher than those of control biofilms ($p < 0.01$) (Fig. 2C).

The control biofilms demonstrated stable specific richness over the 28 days of growth, with 1,004 ± 84 OTUs (Table S4). Interestingly, the Shannon and Pielou indexes significantly increased at D28 ($p < 0.05$), indicating more evenly distributed communities (Table S4). In comparison, the specific richness of biofilms exposed to Co rised at D21, showing a significantly higher number of OTUs and increased Pielou

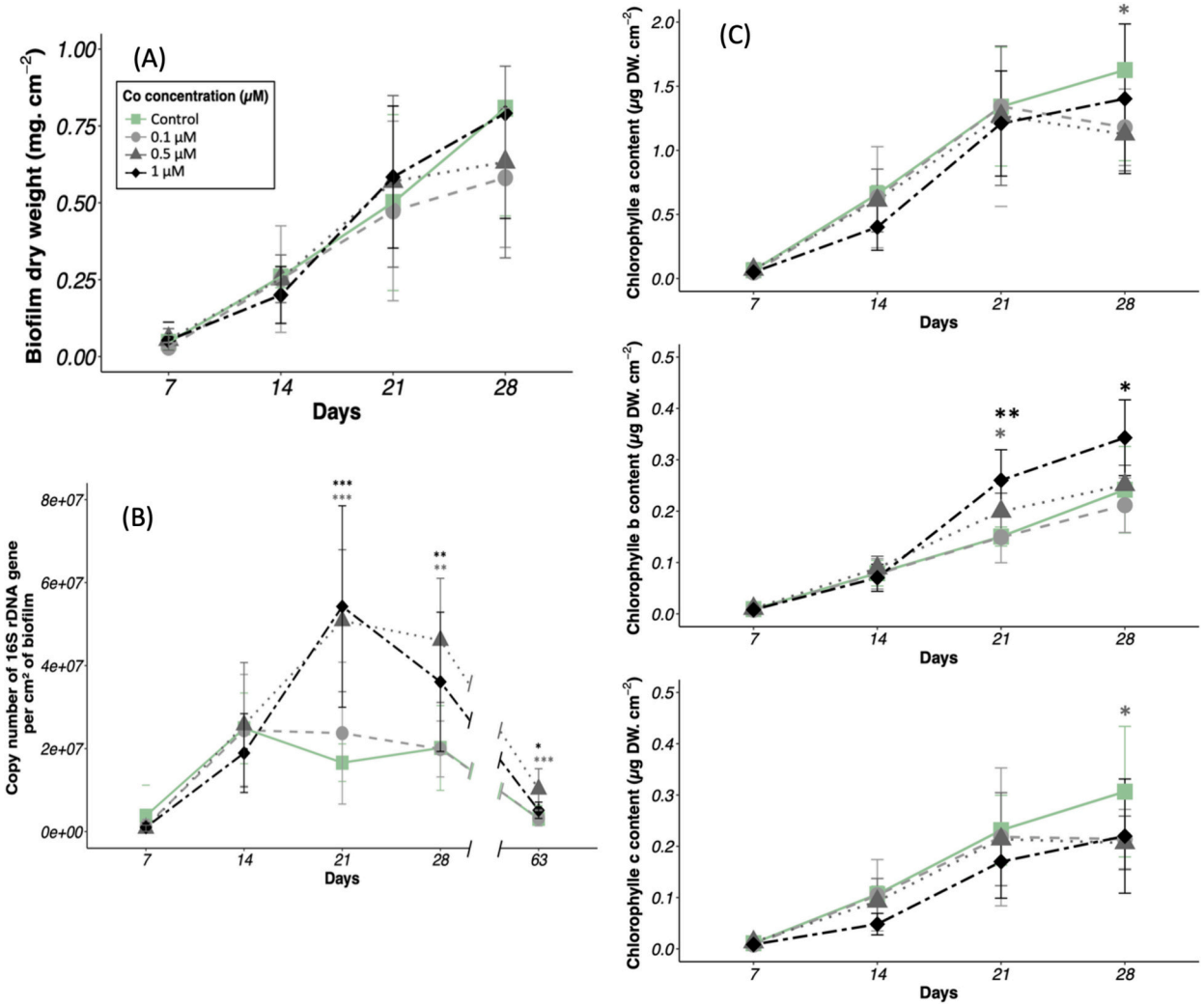

Fig. 2. Main biological parameters of biofilm growing in the different artificial streams exposed to 0, 0.1, 0.5, or 1 μM of Co over time. (A) Dry weight, (B) 16S rDNA gene copy numbers, (C) Chlorophyll *a*, *b*, and *c* contents. Dry weight and chlorophyll content data include samples in one replicate within a stream for Day 7 and Day 14, and two replicates for Day 21 and D28. For 16S rDNA gene copy numbers data includes samples in triplicates within a stream. * indicates statistical differences (* = $p < 0.05$; ** $p < 0.01$), the color of lines (from green to black) indicates the increasing Co concentrations by comparison with control conditions (■: Control conditions; ●: 0.1 μM Co; ▲: 0.5 μM Co; ◆: 1 μM Co).

evenness for 0.5 μM-exposed biofilms ($p < 0.05$) (Table S4). The Chao1 index tracks the rare OTUs within the community, indicating stable richness during colonization under all conditions. However, the exposed biofilms presented higher richness not only at D21 but also at D28 and D63 ($p < 0.05$) (Table S4). Specific richness and the Shannon and Pielou indexes measurably declined in the majority of the biofilms after 35 days of return to natural conditions ($p < 0.001$) (Table S4).

The two-dimensional NMDS ordinations, which were based on Bray-Curtis distances of prokaryotic communities, clustered samples according to the growth time (axis NMDS 1) and Co concentrations (axis NMDS 2) (Fig. 3). All biofilms, including the control, had evolving communities over the biofilm growth period ($p < 0.01$), except biofilms exposed to 0.1 μM Co, which showed no significant variation between D21 and D28 (Table S5). Control biofilms and biofilms treated with 0.1 μM Co exhibited similar community compositions. In contrast, biofilms exposed to 0.5 and 1 μM Co demonstrated significant differences in prokaryotic composition compared to the control or those treated with 0.1 μM, and even between each other, for all sampling periods ($p < 0.01$) (Table S5). Over time, distances between two groups of clusters (Control and 0.1 μM Co vs. 0.5 and 1 μM Co) grew larger, showing that dissimilarities among the biofilms increased. By D63, the biofilm structures remained as different as they were during Co exposure without any cluster overlap (Fig. 3) ($p < 0.005$) (Table S5).

Regardless of the time and Co exposure conditions, biofilms were dominated by *Proteobacteria*, *Bacteroidota*, *Cyanobacteria*, and *Planctomycetota* phyla (Fig. S4-A). *Acidobacteria*, *Actinobacteria*, *Chloroflexi*, and *Verrucomicrobiota* phyla were also found within biofilms, but at a lower percentage. The prokaryotic community of control biofilms at D7 was dominated by *Cyanobacteria* (31.70 ± 25.00%), with their relative abundance decreasing over time to reach 7.00 ± 4.04% of the community by D28 (Fig. 4B, Fig. S4-A). *Bacteroidetes* followed the same trend, with a minimum observed at D21 (Fig. 4B, Fig. S4-A). Conversely, the proportion of *Planctomycetes* increased from D7 to D21 ($p < 0.05$) (Fig. 4B).

Cobalt exposure resulted in a change of major prokaryotic taxa proportions in exposed biofilms (Fig. 4A). The NMDS analysis suggested few alterations in community composition at 0.1 μM of Co (Fig. S5), but we observed significant changes at 0.5 and 1 μM Co (Fig. 4B, Fig. S6). The *Cyanobacteria* was highly sensitive to Co, exhibiting significantly lower proportions compared to the control across all sampling times ($p < 0.05$). By D7, the impact on *Cyanobacteria* was already noticeable, accounting for 5.7 ± 1.5% and 3.5 ± 2.4% of the communities for 0.5 μM and 1 μM-exposed biofilms, respectively (Fig. 4B). Members of the *Planctomycetes* were also adversely affected at 0.5 and 1 μM Co from D14 to D28 ($p < 0.05$). Conversely, *Bacteroidetes* proved highly resistant, accounting for 42.8 ± 3.6% and 36.2 ± 2.7% of the community at D7 and D28 at 1 μM Co. In control biofilms, they represented merely 24.7 ± 9.3% and 14.0 ± 2.5% at D7 and D28, respectively ($p < 0.05$) (Fig. 4B). The *Bacteroidetes* class mainly consisted of *Chitinophagales*, *Flavobacteriales*, and *Sphingobacteriales* orders. By D63, biofilms exposed to 0.5 and 1 μM Co exhibited a significant rise in the relative abundance of *Cyanobacteria* ($p < 0.001$) and a decline for *Bacteroidota* ($p < 0.001$).

3.5. Predicted functional profile of Co-contaminated biofilms

The predicted functional profiles of communities were inferred based on the 16S sequences and PICRUSt2 (Douglas et al., 2020). Picrust2 relies mainly on the accuracy and representativeness of the reference database, which could introduce biases if certain species or functions are underrepresented. In addition, this tool only predicts the presence of functional genes and does not provide information on gene expression levels. These limitations imply that the results obtained must be interpreted cautiously.

The predictive functional potential of biofilms was calculated based on pathways related to biofilm formation and energy metabolisms (photosynthesis, carbon fixation pathways in prokaryotes, methane, nitrogen, and sulfur metabolisms). No variation in the selected pathways was observed between the control and the biofilms exposed to 0.1 μM Co until D21. At this time, photosynthetic and sulfur metabolism potential decreased, while carbon fixation pathways in prokaryotic communities were slightly enhanced ($p < 0.05$) (Fig. S7). For higher Co concentrations (0.5 and 1 μM Co), pathways associated with carbon fixation were influenced by Co from an earlier stage of colonization (D7) ($p < 0.05$) (Fig. S8, Fig. 5). Significantly lower photosynthetic potential was

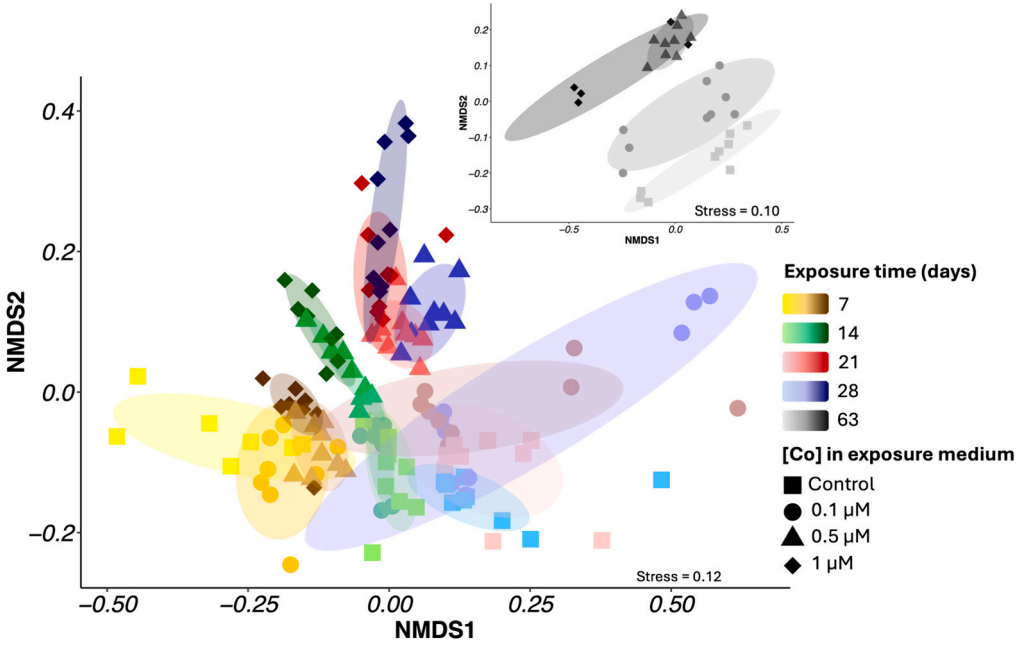

Fig. 3. Non-metric multi-dimensional scaling ordination based on Bray-Curtis dissimilarity matrix of OTUs from prokaryotic communities in growing biofilms in the presence of Co (stress = 0.12). Insert corresponds to NMDS ordination of OTUs at D63 (stress = 0.10). Sampling times are represented as follows: Day 7 (yellow), Day 14 (green), Day 21 (red), Day 28 (blue), and D63 after cessation of Co contamination (Black). Conditions of exposure are represented as follows: ■ Control; • 0.1 μM; ▲0.5 μM; ◆ 1 μM. Ellipses are constructed using the mean and covariance of the group's points, covering 80 % of the points for each group.

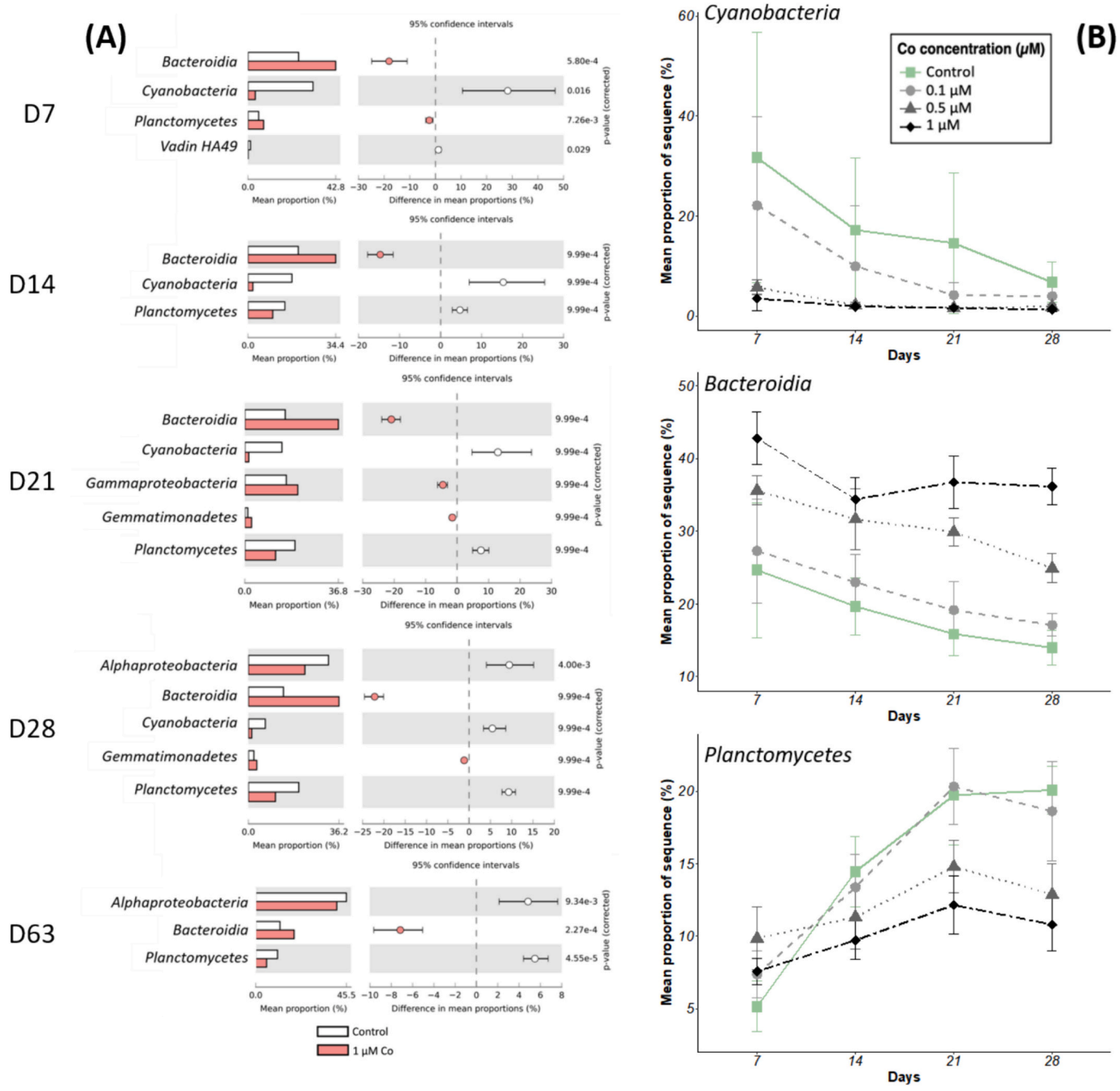

Fig. 4. (A) Mean proportions and differences in mean proportions of taxa with statistically significant differences (White's non-parametric test) between control and 1 µM-exposed biofilms based on STAMP comparison. In white, the control condition; in red, biofilms exposed to 1 µM of Co. (B) Modifications of relative proportions of *Cyanobacteria*, *Bacteroidetes*, and *Planctomycetes* classes within biofilms. The color of lines indicates the increasing Co concentrations by comparison with control conditions (■: Control conditions; ●: 0.1 µM Co; ▲: 0.5 µM Co; ◆: 1 µM Co).

observed, but alternative prokaryotic pathways for carbon fixation were enhanced throughout the entire exposure period ($p < 0.05$). Pathways linked to biofilm formation (including attachment mechanisms and EPS secretion) were negatively impacted in the presence of 0.5 and 1 µM Co from D7 ($p < 0.05$). Similar trends were observed for D14, D21, and D28 (Fig. S8, Fig. 5). There was a significant variation observed for other energy metabolisms related to the methane, sulfur, and nitrogen cycles ($p < 0.05$) but without any clear pattern. Finally, after 35 days of cessation of Co injection, biofilms exposed to 1 µM were able to reach the same levels of photosynthesis and biofilm formation potentials as the control biofilms. Carbon fixation by prokaryotes was still more prevalent in previously exposed biofilms (Fig. 5).

4. Discussion

The present study aimed to evaluate the ecotoxicological impacts of Co on prokaryotic communities in freshwater biofilms and assess their potential to be used as bioindicators of Co contamination in rivers. This is particularly relevant in a context where Co extraction and usage have surged significantly in recent decades (Graedel and Miatto, 2022; U.S Geological Survey, 2018, 2008). Consequently, the health of aquatic ecosystems is endangered due to waste disposal into the environment or the impact from nearby industrial sites (Atibu et al., 2013; Barrio-Parra et al., 2018).

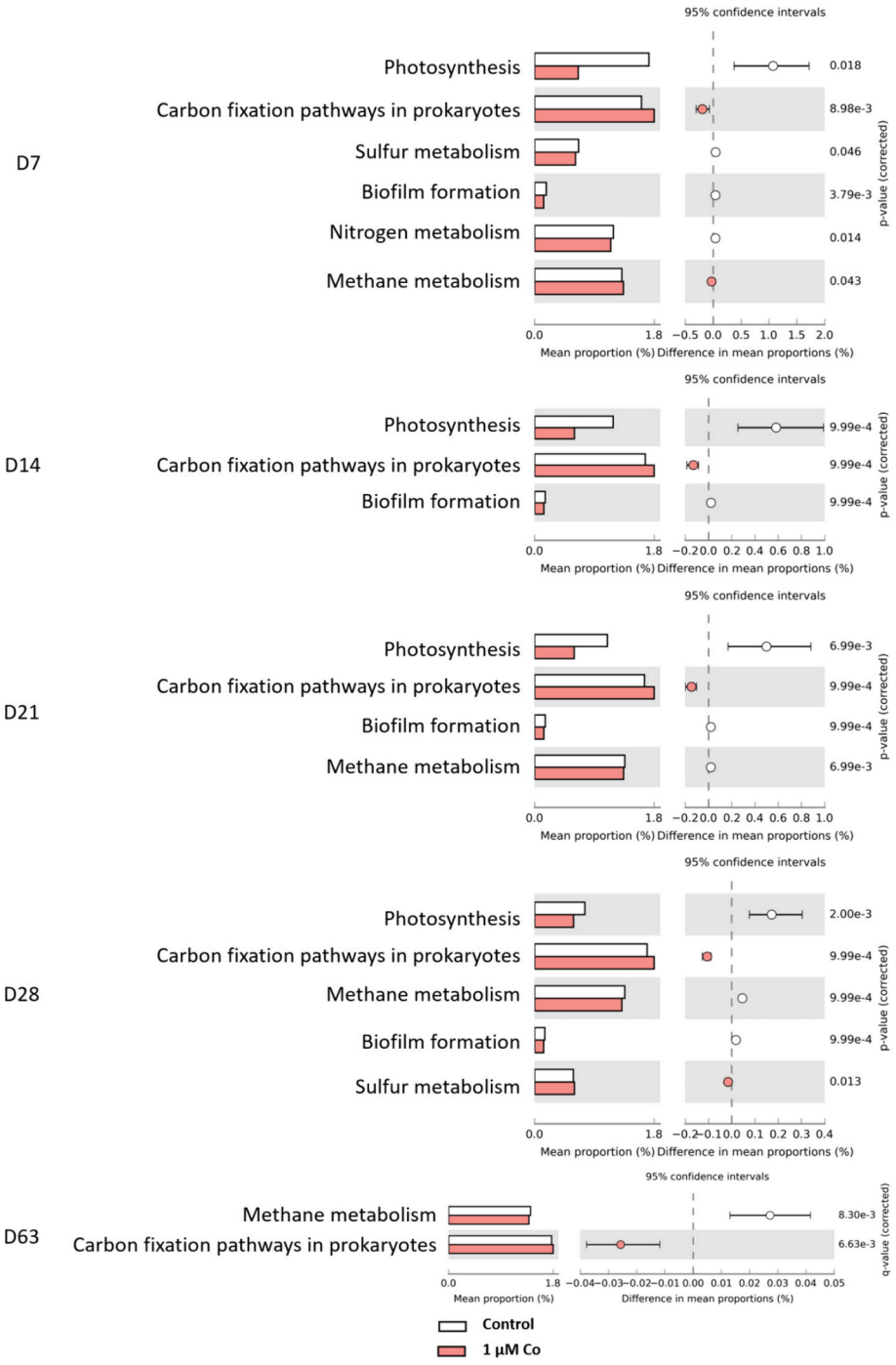

Fig. 5. Predicted functional profile of prokaryotes within control biofilms and biofilms exposed to 1 µM of Co at each sampling time under Co exposure (D7, D14, D21, and D28). Only the mean proportions and differences in mean proportions of pathways with significant differences of relative abundance (STAMPS comparison, White's non-parametric test) are represented. D63: sampling day after 35 days of cessation of Co exposure.

4.1. Cobalt bioaccumulation in growing biofilms as a function of time and ambient concentrations

Cobalt concentrations in growing biofilms showed a good correlation with ambient-free Co^{2+} concentrations, as already observed in recent studies on mature biofilms (Colas et al., 2024; Dutta et al., 2022). Similar correlations were observed for other metals such as Ni, Cd, Zn, and Cu in biofilms, indicating that metal accumulation in biofilms could be a reliable proxy for metal bioavailability (Laderriere et al., 2020; Leguay et al., 2016; Meylan et al., 2004; Morin et al., 2008). While the total accumulated Co levels remained stable during biofilm formation, the internalized fraction gradually increased, accounting for over 80% of the total accumulated Co after 28 days of colonization, irrespective of exposure concentration. This finding concurs with a recent study on mature biofilms, where the intracellular fraction of accumulated Co also increased over time, representing most of the accumulated Co (71 ± 14%) (Colas et al., 2024). After 28 days of 1 µM Co exposure, the levels of intracellular Co measured were consistent with those in previous studies (7.68 ± 1.10 (this study) vs. 8.81 ± 0.45 $\mu mol.g_{DW}^{-1}$ in (Colas et al., 2024)) although Co accumulation was more rapid and substantial in mature biofilms. Higher Co accumulation, when exposed to elevated Co levels, corresponded with higher prokaryotic populations from Day

21 and a distinct microbial composition in biofilms, likely influenced by the selection of tolerant organisms.

4.2. Cobalt impacts on the structure of bacterial community within biofilms

The composition of the prokaryotic community in biofilms from the Gave de Pau River was comparable to those observed in other river biofilms, primarily dominated by the phyla *Proteobacteria*, *Bacteroidota*, *Planctomycetota*, and *Cyanobacteria* (Besemer, 2015; Romaní et al., 2013). The formation of natural biofilms was characterized by a significant increase in the proportions of *Planctomycetota* and a decrease in *Cyanobacteria*, likely related to the decrease in light and temperature from October to December. Biofilms exposed to 0.1 μM Co displayed a similar prokaryotic community abundance, structure, and functional profile to control biofilms.

Structural changes were observed in growing biofilms exposed to 0.5 and 1 μM of Co. While the impact of metals on mature biofilms and microbial communities has been comprehensively described (Colas et al., 2024; Doose et al., 2021; Gil-Allué et al., 2018; Massieux et al., 2004; Morin et al., 2008), our study highlighted the effects of Co on the early stages of biofilm colonization. Dissimilarities in the community compositions were visible by D7, which intensified over exposure time. These differences resulted from shifts in the relative abundance of major taxa as a function of Co concentrations. Among them, *Cyanobacteria* showed a high degree of sensitivity to Co concentrations of 0.5 μM or above. This sensitivity is consistent with previous observations of *Cyanobacteria* in mature environmental biofilms exposed to other metals (Ni, Cu, Zn, and Pb) (Lawrence et al., 2004; Pandey, 2020). On the other hand, as an essential microbial nutrient, a limitation in the growth of an axenic *Cyanobacteria* strain for Co concentrations below 1 nM, has already been confirmed (Facey et al., 2022). This sensitivity underscores the potential for *Cyanobacteria* to serve as a bioindicator of metal contamination. The increased sensitivity of *Cyanobacteria* to Co likely resulted in a reduced photosynthetic potential in the biofilms, as previously reported (Corcoll et al., 2012). Such impacts could affect other heterotrophic bacteria considering that *Cyanobacteria* are significant primary producers in biofilms (Battin et al., 2016). Consequently, the balance between autotrophs and heterotrophs, critical for the functioning of biofilms and carbon cycling in aquatic ecosystems, could be affected. However, the predictive functional analysis in our study suggested that this critical stage of primary production for biofilm formation and maintenance was predominantly supported by non-phototrophic CO_2 fixators. This predicted metabolic redundancy aligns with previous research describing at least six alternatives to photosynthetic organisms for carbon fixation, including members of *Chlorobi*, *Chlorofexi*, *Aquaficea*, *Nitrospira*, *Planctomycetes*, and *Proteobacteria* (Berg, 2011; Garritano et al., 2022; Santos Correa et al., 2023).

A sensitivity to Co was also demonstrated for members of the *Planctomycetes* class. Despite its relative abundance increased over 21 days, it remains half of the abundance in control biofilms. Recent research indicates a decline in the relative abundance of *Planctomycetes* in mature biofilms undergoing exposure to Co concentrations similar to those tested here (Colas et al., 2024). *Planctomycetota* abundances are described to exhibit seasonal variations in river biofilms (Brümmer et al., 2004). Furthermore, a significant association was observed between the *Planctomycetes* class and macroalgal abundances (Lage and Bondoso, 2011). Though macroalgae were not studied in the present research, our data suggest that the absence of resources from photosynthetic primary producers, in the presence of 0.5 and 1 μM Co, triggered a decrease in *Planctomycetota* members. It is noteworthy that certain anaerobic ammonia-oxidizing members of the *Planctomycetota* can perform the reductive acetyl-CoA pathway for carbon fixation, which may serve as an alternative to photosynthesis in this study (Berg, 2011; Ljungdhal, 1986). The acetyl-CoA pathway demands high levels of metals and coenzymes including cobalamin, which is synthesized from Co (Berg, 2011). This suggests that biofilms exposed to high Co concentrations might favor this pathway.

In contrast, *Bacteroidota*, mainly composed of members of *Chitinophagales* and *Flavobacteriales*, were highly resistant and enriched in the presence of Co. *Bacteroidota* has high metabolic diversity and can degrade complex macromolecules. They are important degraders of suspended particles (Besemer, 2016, 2015; Newton et al., 2011). The increase of *Bacteroidetes* in the presence of 0.5 and 1 μM Co may be explained by their ability to degrade more refractory organic molecules within biofilms and ambient waters when labile organic compounds are less prevalent due to *Cyanobacteria* sensitivity to Co.

4.3. Lack of resilience of the prokaryotic community after Co exposure

Our study also investigated the long-term effects of Co contamination following a return to natural water composition. While prevention and detection are crucial, it is also essential to examine the resilience of exposed ecosystems to fully comprehend the impacts of metal contamination. The 35-day period after halting the Co injection did not allow for a complete recovery of the biofilms when compared to the control biofilms. The levels of total bioaccumulated Co decreased but remained up to eight times higher in exposed biofilms than in control biofilms. Similarly, the prokaryotic communities remained different. The incomplete recovery of periphytic diatom communities after contamination with Cd and Zn (Arini et al., 2012) or triclosan (Lawrence et al., 2004) has been previously described. This lack of structural resilience in microbial communities at the base of the trophic chain could have vertical repercussions on the structure and interactions at higher trophic levels (Feckler et al., 2015). Specifically, persistent imbalances in structure and key processes could affect resources and food availability, including oxygen and organic matter, which in turn could disrupt the food web and the ecological status of watercourses.

4.4. Prokaryotic communities are good bioindicators of a co contamination

Even though bacterial communities are key components of ecosystems, they are rarely used as biomonitoring tools. Microorganisms are recognized for their significant bioindication potential, as they are sensitive to environmental shifts (Doose et al., 2021; Lear et al., 2009; Zhang et al., 2019). Their activity and position at the basis of the trophic chain also enables them to function as a early warning tool before higher trophic levels show any repercussions. This study aimed to assess the ability of prokaryotic communities to act as a bioindicator of Co exposure. Microorganisms displayed a swift response, with major taxa such as *Cyanobacteria* and *Planctomycetes* showing sensitivity, and others, like *Bacteroidetes*, exhibiting resistance to Co. Further, utilizing a molecular approach to target prokaryotic communities facilitates the potential prediction of functional implications linked to exposure to a contaminant. This approach could also be advantageous for assessing the restoration of aquatic ecosystems since Co contamination history was still evident in the prokaryotic community structure even after the stress induction period and an exposure period without the contaminant had concluded. Therefore, the prokaryotic communities assessed in this study offer compelling evidence as viable alternatives to traditional counting methods and morphological analyses, which are often compromised by human biases (Haase et al., 2010). Indeed, microbial approaches are less time-consuming and labor-intensive if applied as a routine method. An additional advantage is that they present a comprehensive view of the impacts of river contamination, from community structure and group interactions to predicted functional profile, providing further insight into potential repercussions at higher trophic levels and even at the ecosystem level.

According to the definition provided by the IUPAC (Duffus et al., 2007), prokaryotic communities that develop within river biofilms are suitable bioindicators. They can be used alone or integrated with other

physical, chemical, and biological measures in a modeling approach to better understand metal impacts on environmental health (Astudillo-García et al., 2019). When developing a new monitoring tool based on these bacterial communities, one must address the challenge of characterizing local reference communities. This is because water composition, which can impact the natural composition of bacterial communities within river biofilms, can vary depending on seasons, river conditions, and geography.

Further studies focusing on the sensitive and resistant groups, as described in the present work, are needed to confirm their behavior in the presence of metals. Additionally, the interactions between all compartments within biofilms, including microalgae, should be considered in future assessments of metal impact on the first levels of aquatic and terrestrial food webs.

Funding

This research was funded by the Partnership Chair E2S-UPPA-TotalEnergies-Rio Tinto (ANR-16-IDEX-0002).

CRediT authorship contribution statement

Sarah Gourgues: Writing – review & editing, Writing – original draft, Visualization, Validation, Software, Methodology, Investigation, Formal analysis, Data curation, Conceptualization. **Marisol Goñi-Urriza:** Writing – review & editing, Writing – original draft, Validation, Supervision, Investigation, Conceptualization. **Mathieu Milhe-Poutingon:** Investigation, Formal analysis. **Patrick Baldoni-Andrey:** Writing – review & editing, Resources, Funding acquisition. **Nicholas Bagger Gurieff:** Writing – review & editing, Resources, Funding acquisition. **Clémentine Gelber:** Writing – review & editing, Resources, Project administration. **Séverine Le Faucheur:** Writing – review & editing, Writing – original draft, Validation, Supervision, Resources, Project administration, Investigation, Funding acquisition, Conceptualization.

Declaration of competing interest

The authors declare that they have no known competing financial interests or personal relationships that could have appeared to influence the work reported in this paper.

Data availability

Data will be made available on request.

Acknowledgment

We thank the members of TotalEnergies Environment & Sustainable Development Team at Pôle d'Études et de Recherches (PERL, Lacq, France) for the access to Pilot Rivers facilities and experimental assistance during the mesocosm experiment. Amplicon sequencing was performed by PGTB (Bordeaux, France) with the assistance of Zoé Delporte and Erwan Guichoux. We also thank Claire Gassie (Université de Pau et des Pays de l'Adour, E2S-UPPA, CNRS, IPREM, Pau, France) for her technical assistance during laboratory work and characterization of microbial communities.

Appendix A. Supplementary data

Supplementary data to this article can be found online at https://doi.org/10.1016/j.scitotenv.2024.175713.

References

Allen, L.H., 2012. Vitamin B-12. Adv. Nutr. 3, 54–55. https://doi.org/10.3945/an.111.001370.

Arini, A., Feurtet-Mazel, A., Maury-Brachet, R., Pokrovsky, O.S., Coste, M., Delmas, F., 2012. Recovery potential of periphytic biofilms translocated in artificial streams after industrial contamination (Cd and Zn). Ecotoxicology 21, 1403–1414. https://doi.org/10.1007/s10646-012-0894-3.

Astudillo-García, C., Hermans, S.M., Stevenson, B., Buckley, H.L., Lear, G., 2019. Microbial assemblages and bioindicators as proxies for ecosystem health status: potential and limitations. Appl. Microbiol. Biotechnol. 103, 6407–6421. https://doi.org/10.1007/s00253-019-09963-0.

Atibu, E.K., Devarajan, N., Thevenon, F., Mwanamoki, P.M., Tshibanda, J.B., Mpiana, P. T., Prabakar, K., Mubedi, J.I., Wildi, W., Poté, J., 2013. Concentration of metals in surface water and sediment of Luilu and Musonoie Rivers, Kolwezi-Katanga, Democratic Republic of Congo. Appl. Geochem. 39, 26–32. https://doi.org/10.1016/j.apgeochem.2013.09.021.

Banza Lubaba Nkulu, C., Casas, L., Haufroid, V., De Putter, T., Saenen, N.D., Kayembe-Kitenge, T., Musa Obadia, P., Kyanika Wa Mukoma, D., Lunda Ilunga, J.-M., Nawrot, T.S., Luboya Numbi, O., Smolders, E., Nemery, B., 2018. Sustainability of artisanal mining of cobalt in DR Congo. Nat. Sustain. 1, 495–504. https://doi.org/10.1038/s41893-018-0139-4.

Barrio-Parra, F., Elío, J., De Miguel, E., García-González, J.E., Izquierdo, M., Álvarez, R., 2018. Environmental risk assessment of cobalt and manganese from industrial sources in an estuarine system. Environ. Geochem. Health 40, 737–748. https://doi.org/10.1007/s10653-017-0020-9.

Batista, M.J., Bidovec, M., Demetriades, A., De Vivo, B., De Vos, W., Duris, M., Gilucis, A., Gregorauskiene, V., Halamic, J., Heitzmann, P., Lima, A., Jordan, G., Klaver, G., Klein, P., Lis, J., Locutura, J., Marsina, K., Mazreku, A., O'Connor, P.J., Olsson, S., Ottesen, R.-T., Petersell, V., Plant, J.A., Reeder, S., Salpeteur, I., Sandström, H., Siewers, U., Steenfelt, A., Tarvainen, T., Salminen, R., 2005. Geochemical Atlas of Europe. Part 1: Background Information, Methodology and Maps. Geological Survey of Finland, Espoo.

Battin, T.J., Besemer, K., Bengtsson, M.M., Romani, A.M., Packmann, A.I., 2016. The ecology and biogeochemistry of stream biofilms. Nat. Rev. Microbiol. 14, 251–263. https://doi.org/10.1038/nrmicro.2016.15.

Berg, I.A., 2011. Ecological aspects of the distribution of different autotrophic CO_2 fixation pathways. Appl. Environ. Microbiol. 77, 1925–1936. https://doi.org/10.1128/AEM.02473-10.

Besemer, K., 2015. Biodiversity, community structure and function of biofilms in stream ecosystems. Res. Microbiol. 166, 774–781. https://doi.org/10.1016/j.resmic.2015.05.006.

Besemer, K., 2016. Microbial biodiversity in natural biofilms. In: Aquatic Biofilms: Ecology, Water Quality and Wastewater Treatment. Caister Academic Press, pp. 63–88. https://doi.org/10.21775/9781910190173.04.

Bokulich, N.A., Subramanian, S., Faith, J.J., Gevers, D., Gordon, J.I., Knight, R., Mills, D. A., Caporaso, J.G., 2013. Quality-filtering vastly improves diversity estimates from Illumina amplicon sequencing. Nat. Methods 10, 57–59. https://doi.org/10.1038/nmeth.2276.

Brümmer, I.H.M., Felske, A.D.M., Wagner-Döbler, I., 2004. Diversity and seasonal changes of uncultured *Planctomycetales* in river biofilms. Appl. Environ. Microbiol. 70, 5094–5101. https://doi.org/10.1128/AEM.70.9.5094-5101.2004.

Bryan, S.E., Tipping, E., Hamilton-Taylor, J., 2002. Comparison of measured and modelled copper binding by natural organic matter in freshwaters. Comp. Biochem. Physiol., Part C: Toxicol. Pharmacol. 133, 37–49. https://doi.org/10.1016/S1532-0456(02)00083-2.

Chen, B.-Y., Wu, C.-H., Chang, J.-S., 2006. An assessment of the toxicity of metals to Pseudomonas aeruginosa PU21 (Rip64). Bioresour. Technol. 97, 1880–1886. https://doi.org/10.1016/j.biortech.2005.08.022.

Colas, S., Marie, B., Morin, S., Milhe-Poutingon, M., Foucault, P., Chalvin, S., Gelber, C., Baldoni-Andrey, P., Gurieff, N., Fortin, C., Le Faucheur, S., 2024. New sensitive tools to characterize meta-metabolome response to short- and long-term cobalt exposure in dynamic river biofilm communities. Sci. Total Environ., 171851 https://doi.org/10.1016/j.scitotenv.2024.171851.

Corcoll, N., Bonet, B., Morin, S., Tlili, A., Leira, M., Guasch, H., 2012. The effect of metals on photosynthesis processes and diatom metrics of biofilm from a metal-contaminated river: a translocation experiment. Ecol. Indic. 18, 620–631. https://doi.org/10.1016/j.ecolind.2012.01.026.

Coste, M., Boutry, S., Tison-Rosebery, J., Delmas, F., 2009. Improvements of the biological diatom index (BDI): description and efficiency of the new version (BDI-2006). Ecol. Indic. 9, 621–650. https://doi.org/10.1016/j.ecolind.2008.06.003.

Doose, C., Morin, S., Malbezin, L., Vedrenne, J., Fortin, C., 2021. Effects of thorium on bacterial, microalgal and micromeiofaunal community structures in a periphytic biofilm. Ecotoxicol. Environ. Saf. 218, 112276 https://doi.org/10.1016/j.ecoenv.2021.112276.

Douglas, G.M., Maffei, V.J., Zaneveld, J.R., Yurgel, S.N., Brown, J.R., Taylor, C.M., Huttenhower, C., Langille, M.G.I., 2020. PICRUSt2 for prediction of metagenome functions. Nat. Biotechnol. 38, 685–688. https://doi.org/10.1038/s41587-020-0548-6.

Duffus, J.H., Nordberg, M., Templeton, D.M., 2007. Glossary of terms used in toxicology, 2nd edition (IUPAC recommendations 2007). Pure Appl. Chem. 79, 1153–1344. https://doi.org/10.1351/pac200779071153.

Dulay, H., Tabares, M., Kashefi, K., Reguera, G., 2020. Cobalt resistance via detoxification and mineralization in the iron-reducing bacterium *Geobacter sulfurreducens*. Front. Microbiol. 11, 600463 https://doi.org/10.3389/fmicb.2020.600463.

Dutta, A., Mandal, A., Chanda, P., Misra, S., Mukherjee, J., Das, R., 2022. Biosorption of cadmium and cobalt by intertidal multicomponent biofilms. Mar. Pollut. Bull. 185, 114318 https://doi.org/10.1016/j.marpolbul.2022.114318.

El-Sheekh, M.M., El-Naggar, A.H., Osman, M.E.H., El-Mazaly, E., 2003. Effect of cobalt on growth, pigments and the photosynthetic electron transport in *Monoraphidium minutum* and *Nitzchia perminuta*. Braz. J. Plant Physiol. 15, 159–166. https://doi.org/10.1590/S1677-04202003000300005.

Environment Canada, 2017. Federal Environmental Quality Guidelines (FEQG) - cobalt. https://www.canada.ca/en/environment-climate-change/services/evaluating-existing-substances/canadian-environmental-protection-act-1999-federal-environmental-quality-guidelines-cobalt.html (accessed 15 May 2024).

Escudié, F., Auer, L., Bernard, M., Mariadassou, M., Cauquil, L., Vidal, K., Maman, S., Hernandez-Raquet, G., Combes, S., Pascal, G., 2018. FROGS: find, rapidly, OTUs with galaxy solution. Bioinformatics 34, 1287–1294. https://doi.org/10.1093/bioinformatics/btx791.

European Chemical Agency (ECHA), 2023. Registration dossier - cobalt. https://echa.europa.eu/fr/registration-dossier/-/registered-dossier/15506/6/2/6 (accessed 27 September 2023).

Facey, J.A., King, J.J., Apte, S.C., Mitrovic, S.M., 2022. Assessing the importance of cobalt as a micronutrient for freshwater *Cyanobacteria*. J. Phycol. 58, 71–79. https://doi.org/10.1111/jpy.13216.

Fawzy, M.A., Hifney, A.F., Adam, M.S., Al-Badaani, A.A., 2020. Biosorption of cobalt and its effect on growth and metabolites of *Synechocystis pevalekii* and *Scenedesmus bernardii*: isothermal analysis. Environ. Technol. Innov. 19, 100953 https://doi.org/10.1016/j.eti.2020.100953.

Feckler, A., Kahlert, M., Bundschuh, M., 2015. Impacts of contaminants on the ecological role of lotic biofilms. Bull. Environ. Contam. Toxicol. 95, 421–427. https://doi.org/10.1007/s00128-015-1642-1.

Flemming, H.-C., Wingender, J., 2010. The biofilm matrix. Nat. Rev. Microbiol. 8, 623–633. https://doi.org/10.1038/nrmicro2415.

Garritano, A.N., Song, W., Thomas, T., 2022. Carbon fixation pathways across the bacterial and archaeal tree of life. PNAS Nexus 1, pgac226. https://doi.org/10.1093/pnasnexus/pgac226.

Gikas, P., 2008. Single and combined effects of nickel (Ni(II)) and cobalt (Co(II)) ions on activated sludge and on other aerobic microorganisms: a review. J. Hazard. Mater. 159, 187–203. https://doi.org/10.1016/j.jhazmat.2008.02.048.

Gil-Allué, C., Tlili, A., Schirmer, K., Gessner, M.O., Behra, R., 2018. Long-term exposure to silver nanoparticles affects periphyton community structure and function. Environ. Sci. Nano 5, 1397–1407. https://doi.org/10.1039/C8EN00132D.

Graedel, T.E., Miatto, A., 2022. U.S. cobalt: a cycle of diverse and important uses. Resour. Conserv. Recycl. 184, 106441 https://doi.org/10.1016/j.resconrec.2022.106441.

Guasch, H., Ricart, M., López-Doval, J., Bonnineau, C., Proia, L., Morin, S., Muñoz, I., Romaní, A.M., Sabater, S., 2016. Influence of grazing on triclosan toxicity to stream periphyton. Freshw. Biol. 61, 2002–2012. https://doi.org/10.1111/fwb.12797.

Haase, P., Pauls, S.U., Schindehütte, K., Sundermann, A., 2010. First audit of macroinvertebrate samples from an EU water framework directive monitoring program: human error greatly lowers precision of assessment results. J. N. Am. Benthol. Soc. 29, 1279–1291. https://doi.org/10.1899/09-183.1.

Hang, M.N., Gunsolus, I.L., Wayland, H., Melby, E.S., Mensch, A.C., Hurley, K.R., Pedersen, J.A., Haynes, C.L., Hamers, R.J., 2016. Impact of nanoscale Lithium nickel manganese cobalt oxide (NMC) on the bacterium *Shewanella oneidensis* MR-1. Chem. Mater. 28, 1092–1100. https://doi.org/10.1021/acs.chemmater.5b04505.

Hassen, A., Saidi, N., Cherif, M., Boudabous, A., 1998. Resistance of environmental bacteria to heavy metals. Bioresour. Technol. 64, 7–15. https://doi.org/10.1016/S0960-8524(97)00161-2.

Institut national de l''environnement industriel et des risques, 2022. Substances Pertinentes à Surveiller (SPAS) dans les eaux de surface - Etude des données à l'échelle des bassins hydrographiques et selon les types de pression chimique (No. Ineris-203220-2733069-v2.0). Ineris, Verneuil-en-Halatte.

Ivorra, N., Bremer, S., Guasch, H., Kraak, M.H.S., Admiraal, W., 2000. Differences in the sensitivity of benthic microalgae to ZN and CD regarding biofilm development and exposure history. Environ. Toxicol. Chem. 19, 1332–1339. https://doi.org/10.1002/etc.5620190516.

Laderriere, V., Paris, L.-E., Fortin, C., 2020. Proton competition and free ion activities drive cadmium, copper, and nickel accumulation in river biofilms in a Nordic ecosystem. Environments 7, 112. https://doi.org/10.3390/environments7120112.

Lage, O.M., Bondoso, J., 2011. Planctomycetes diversity associated with macroalgae: Planctomycetes-macroalgae diversity. FEMS Microbiol. Ecol. 78, 366–375. https://doi.org/10.1111/j.1574-6941.2011.01168.x.

Lawrence, J.R., Chenier, M.R., Roy, R., Beaumier, D., Fortin, N., Swerhone, G.D.W., Neu, T.R., Greer, C.W., 2004. Microscale and molecular assessment of impacts of nickel, nutrients, and oxygen level on structure and function of river biofilm communities. Appl. Environ. Microbiol. 70, 4326–4339. https://doi.org/10.1128/AEM.70.7.4326-4339.2004.

Lear, Gavin, Niyogi, D., Harding, J., Dong, Y., Lewis, G., 2009. Biofilm bacterial community structure in streams affected by acid mine drainage. Appl. Environ. Microbiol. 75, 3455–3460. https://doi.org/10.1128/AEM.00274-09.

Lee, L.H., Lustigman, B., Chu, I.-Y., Hsu, S., 1992. Effect of lead and cobalt on the growth of Anacystis nidulans. Bull. Environ. Contam. Toxicol. 48 https://doi.org/10.1007/BF00194376.

Leguay, S., Lavoie, I., Levy, J.L., Fortin, C., 2016. Using biofilms for monitoring metal contamination in lotic ecosystems: the protective effects of hardness and pH on metal bioaccumulation. Environ. Toxicol. Chem. 35, 1489–1501. https://doi.org/10.1002/etc.3292.

Li, M., Zhu, Q., Hu, C., Chen, L., Liu, Z., Kong, Z., 2007. Cobalt and manganese stress in the microalga Pavlova viridis (Prymnesiophyceae): effects on lipid peroxidation and antioxidant enzymes. J. Environ. Sci. 19, 1330–1335. https://doi.org/10.1016/S1001-0742(07)60217-4.

Li, K., Qian, J., Wang, P., Wang, C., Lu, B., Jin, W., He, X., Tang, S., Zhang, C., Gao, P., 2020. Responses of freshwater biofilm formation processes (from colonization to maturity) to anatase and rutile TiO_2 nanoparticles: effects of nanoparticles aging and transformation. Water Res. 182, 115953 https://doi.org/10.1016/j.watres.2020.115953.

Ljungdhal, L.G., 1986. The autotrophic pathway of acetate synthesis in acetogenic bacteria. Annu. Rev. Microbiol. 40, 415–450. https://doi.org/10.1146/annurev.mi.40.100186.002215.

Mahé, F., Rognes, T., Quince, C., De Vargas, C., Dunthorn, M., 2014. Swarm: robust and fast clustering method for amplicon-based studies. PeerJ 2, e593. https://doi.org/10.7717/peerj.593.

Martens, H., Barg, M., Warren, D., Jah, J.-H., 2002. Microbial production of vitamin B 12. Appl. Microbiol. Biotechnol. 58, 275–285. https://doi.org/10.1007/s00253-001-0902-7.

Martinez Arbizu, P.R., 2020. Package version 0.4 (pairwiseAdonis: pairwise multilevel comparison using adonis). https://github.com/pmartinezarbizu/pairwiseAdonis.

Massieux, B., Boivin, M.E.Y., van den Ende, F.P., Langenskiöld, J., Marvan, P., Barranguet, C., Admiraal, W., Laanbroek, H.J., Zwart, G., 2004. Analysis of structural and physiological profiles to assess the effects of cu on biofilm microbial communities. Appl. Environ. Microbiol. 70, 4512–4521. https://doi.org/10.1128/AEM.70.8.4512-4521.2004.

McGeer, J., Henningsen, G., Lanno, R., Fisher, N., Sappington, K., Drexler, J., Beringer, M., 2004. Issue Paper on the Bioavailability and Bioaccumulation of Metals. US Environ. Prot. Agency.

Meylan, S., Behra, R., Sigg, L., 2004. Influence of metal speciation in natural freshwater on bioaccumulation of copper and zinc in Periphyton: a microcosm study. Environ. Sci. Technol. 38, 3104–3111. https://doi.org/10.1021/es034993n.

Morin, S., Duong, T.T., Herlory, O., Feurtet-Mazel, A., Coste, M., 2008. Cadmium toxicity and bioaccumulation in freshwater biofilms. Arch. Environ. Contam. Toxicol. 54, 173–186. https://doi.org/10.1007/s00244-007-9022-4.

Newton, R.J., Jones, S.E., Eiler, A., McMahon, K.D., Bertilsson, S., 2011. A guide to the natural history of freshwater lake bacteria. Microbiol. Mol. Biol. Rev. 75, 14–49. https://doi.org/10.1128/MMBR.00028-10.

Oksanen, J., Simpson, G., Blanchet, F., Kindt, R., Legendre, P., Minchin, P., O'Hara, R., Solymos, P., Stevens, M., Szoecs, E., Wagner, H., Barbour, M., Bedward, M., Bolker, B., Borcard, D., Carvalho, G., Chirico, M., De Caceres, M., Durand, S., Evangelista, H., FitzJohn, R., Friendly, M., Furneaux, B., Hannigan, G., Hill, M., Lahti, L., McGlinn, D., Ouellette, M., Ribeiro, Cunha E., Smith, T., Stier, A., Ter Braak, C., Weedon, J., 2022. Vegan: community ecology package. R package version 2.6–4. https://CRAN.R-project.org/package=vegan.

Pal, A., Bhattacharjee, S., Saha, J., Sarkar, M., Mandal, P., 2022. Bacterial survival strategies and responses under heavy metal stress: a comprehensive overview. Crit. Rev. Microbiol. 48, 327–355. https://doi.org/10.1080/1040841X.2021.1970512.

Pandey, L.K., 2020. In situ assessment of metal toxicity in riverine periphytic algae as a tool for biomonitoring of fluvial ecosystems. Environ. Technol. Innov. 18, 100675 https://doi.org/10.1016/j.eti.2020.100675.

Parks, D.H., Tyson, G.W., Hugenholtz, P., Beiko, R.G., 2014. STAMP: statistical analysis of taxonomic and functional profiles. Bioinformatics 30, 3123–3124. https://doi.org/10.1093/bioinformatics/btu494.

Rognes, T., Flouri, T., Nichols, B., Quince, C., Mahé, F., 2016. VSEARCH: a versatile open source tool for metagenomics. PeerJ 4, e2584. https://doi.org/10.7717/peerj.2584.

Romaní, A.M., Amalfitano, S., Artigas, J., Fazi, S., Sabater, S., Timoner, X., Ylla, I., Zoppini, A., 2013. Microbial biofilm structure and organic matter use in mediterranean streams. Hydrobiologia 719, 43–58. https://doi.org/10.1007/s10750-012-1302-y.

Sabater, S., Guasch, H., Ricart, M., Romaní, A., Vidal, G., Klünder, C., Schmitt-Jansen, M., 2007. Monitoring the effect of chemicals on biological communities. The biofilm as an interface. Anal. Bioanal. Chem. 387, 1425–1434. https://doi.org/10.1007/s00216-006-1051-8.

Santos Correa, S., Schultz, J., Lauersen, K.J., Soares Rosado, A., 2023. Natural carbon fixation and advances in synthetic engineering for redesigning and creating new fixation pathways. J. Adv. Res. 47, 75–92. https://doi.org/10.1016/j.jare.2022.07.011.

Tipping, E., 2007. Modelling the interactions of hg(II) and methylmercury with humic substances using WHAM/model VI. Appl. Geochem. 22, 1624–1635. https://doi.org/10.1016/j.apgeochem.2007.03.021.

U.S Geological Survey, 2008. Mineral Commodity Summaries 2008: U.S Geological Survey. https://doi.org/10.3133/mineral2008.

U.S Geological Survey, 2018. Mineral Commodity Summaries 2018: U.S Geological Survey. https://doi.org/10.3133/mineral2008.

Wang, Y., Qian, P.-Y., 2009. Conservative fragments in bacterial 16S rRNA genes and primer design for 16S ribosomal DNA amplicons in metagenomic studies. PloS One 4, e7401. https://doi.org/10.1371/journal.pone.0007401.

Yang, C., Mai, J., Cao, X., Burberry, A., Cominelli, F., Zhang, L., 2023. ggpicrust2: an R package for PICRUSt2 predicted functional profile analysis and visualization. Bioinformatics 39, btad470. https://doi.org/10.1093/bioinformatics/btad470.

Zhang, Xiaohui, Tang, S., Wang, M., Sun, W., Xie, Y., Peng, H., Zhong, A., Liu, H., Zhang, Xiaowei, Yu, H., Giesy, J.P., Hecker, M., 2019. Acid mine drainage affects the diversity and metal resistance gene profile of sediment bacterial community along a river. Chemosphere 217, 790–799. https://doi.org/10.1016/j.chemosphere.2018.10.210.